

Figure 1. Electronic spectra of a mixture of **1** (1 mM) and **2a** (2 mM) in water (pH 6.5) at different temperatures.

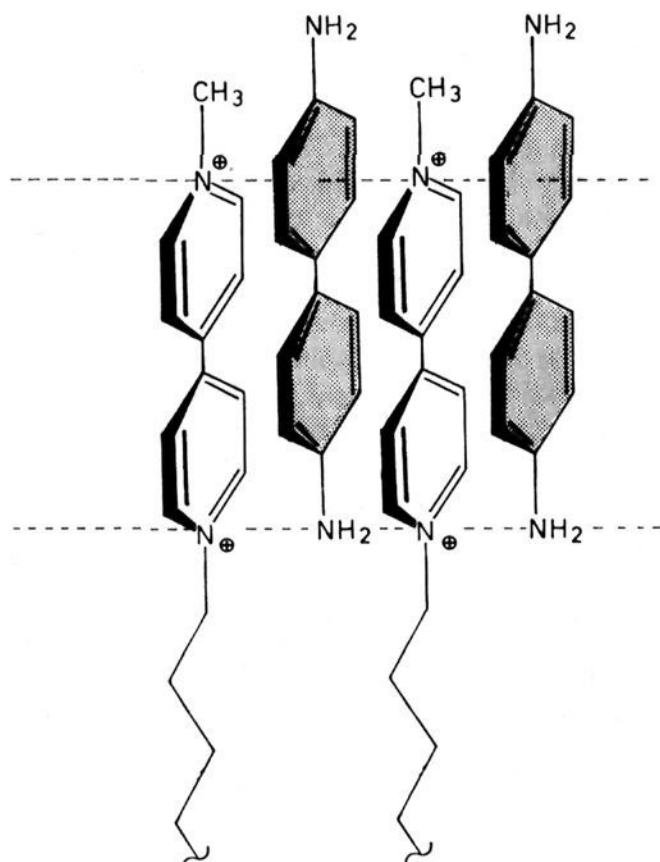


Figure 2. Model of the blue aggregate between **1** and **2a**. The broken lines connect the supposed electron-donating and -accepting centers.

transfer occurs. Less dramatic reversible spectroscopic shifts have been observed earlier.<sup>9</sup> They occur around the phase transition temperature of the hydrophobic membrane. This is not the case with the molecular complex of Figure 2. The temperature at which the color change is observed rather depends on counterions, solubility, and surface charges of guest vesicles. A vesicular charge-transfer complex has also been described earlier,<sup>10</sup> but its absorption spectrum does not change significantly with temperature.

The formation of the blue complex of aggregated paraquat amphiphiles is also useful for the proof of domain formation in host vesicle membranes. **1** was dissolved in dipalmitoyl phos-

phatidylcholine vesicles in a molar ratio of 1:10. Addition of benzidine gave no blue color at room temperature or 0 °C. After addition of sodium perchlorate at 35 °C and short sonication to circumvent precipitation, however, a strong 615-nm absorption band was again observed at room temperature, which disappeared at 70 °C.

The appearance of long-wavelength bands in vesicular systems is probably not limited to membranes having bipyridinium head groups. We expect similar phenomena with analogous systems, e.g., benzidine head groups and paraquat monomers, hydrophilic quinone head groups and hydroquinone monomers, etc. Work along this line is in progress.

**Acknowledgment.** This research was supported by grants from the Deutsche Forschungsgemeinschaft, the Fonds der Chemischen Industrie, and the Förderungskommission für Forschung der Freien Universität Berlin (FGS Biomembranen).

### Controlled Modification of Organic Polymer Surfaces by Continuous Wave Far-Ultraviolet (185 nm) and Pulsed-Laser (193 nm) Radiation: XPS Studies

Sylvain Lazare,<sup>†</sup> Peter D. Hoh, John M. Baker, and R. Srinivasan\*

IBM Thomas J. Watson Research Center  
Yorktown Heights, New York 10598

Received April 5, 1984

Modification of polymer surfaces to improve adhesion or biocompatibility or to provide functionalities for further reaction is an attractive goal.<sup>1,2</sup> Of the various techniques<sup>3,4</sup> that have been considered so far for this purpose, photochemistry has received little attention.<sup>2,5,6</sup> IR and XPS studies of polymer surface oxidation brought about by radiation of wavelength greater than 200 nm have been reported,<sup>7,8</sup> but these were mainly concerned with the photostability of the polymers.

In contrast to radiation >200 nm, far-ultraviolet offers several attractive features for the modification of polymer surfaces: (i) Nearly all polymers absorb intensely and penetration of the radiation (95% absorption) is limited to a depth of 3000 Å.<sup>9</sup> Therefore, the absorption of the photons in the polymer is confined to the diffusion depth of the gas molecules, resulting in high efficiency for the reaction. (ii) The high quantum yield for bond breaking results in short exposure times: upon exposure to 2.5 mW/cm<sup>2</sup> at 185 nm from a mercury resonance lamp, the maximum change in surface composition as monitored by XPS occurs in just a few minutes. Modification of the polymer surface by ablative photodecomposition<sup>9</sup> with a pulsed 193-nm ArF laser results in the creation of a fresh surface with a novel composition.

<sup>†</sup> Permanent address: L.A. 348 du C.N.R.S., University of Bordeaux I, 33405 Talence Cedex, France.

(1) Mittal, K. L. "Physicochemical Aspects of Polymer Surfaces"; New York: Plenum Press, 1983. Lyman, D. J. *Angew. Chem., Int. Ed. Engl.* **1974**, *13*, 108.

(2) Tazuke, S.; Kimura, H. *Makromol. Chem.* **1978**, *179*, 2603.

(3) Chromic acid etching, see: (a) Rasmussen, J. R.; Stedronsky, E. R.; Whitesides, G. M. *J. Am. Chem. Soc.* **1977**, *99*, 4782. (b) Rasmussen, J. R.; Bergbreiter, D. E.; Whitesides, G. M. *Ibid.* **1977**, *99*, 4740.

(4) Plasma treatments, see: (a) Briggs, D.; Rauce, D. G.; Kendall, C. R.; Blythe, A. R. *Polymer* **1980**, *21*, 895. (b) Clark, D. T. In "Polymer Surfaces"; Clark, D. T., Feast, W. J., Eds.; Wiley: London, 1978. (c) Yasuda, H.; Marsh, H. C.; Brandt, S.; Reilley, C. N. *J. Polym. Sci.* **1977**, *15*, 991. (d) Amouroux, J.; Goldman, M.; Revoil, M. F. *J. Polym. Sci.* **1982**, *19*, 1373.

(5) Owens, D. K. *J. Appl. Polym. Sci.* **1975**, *19*, 3315.

(6) (a) Peeling, J.; Clark, D. T. *J. Appl. Polym. Sci.* **1981**, *26*, 3761; *J. Polym. Sci.* **1984**, *22*, 419.

(7) Blais, P.; Day, M.; Wiles, D. M. *J. Appl. Polym. Sci.* **1973**, *17*, 1895.

(8) Peeling, J.; Clark, D. T. *Polymer Degradation Stab.* **1981**, *3*, 92, 177.

(9) Srinivasan, R.; Leigh, W. J. *J. Am. Chem. Soc.* **1982**, *104*, 6784.

(9) (a) Russell, J. C.; Costa, S. B.; Seiders, R. P.; Whitten, D. G. *J. Am. Chem. Soc.* **1980**, *102*, 5678. (b) Nakashima, N.; Kunitake, T. *J. Am. Chem. Soc.* **1982**, *104*, 4261.

(10) Murakami, Y.; Nakano, A. *J. Am. Chem. Soc.* **1982**, *104*, 2937.

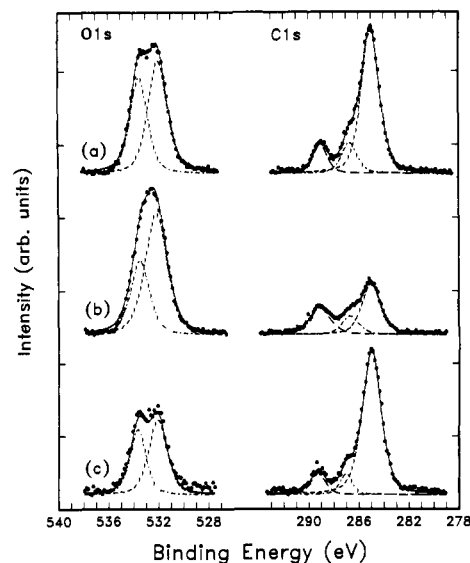


**Figure 1.** XPS spectrum of poly(ethylene terephthalate) surfaces (a) as received (the assignment of the individual peaks is as follows: C 1s, 285.0 eV aromatic carbon, 286.8 eV carbon bearing a single oxygen, 289.0 eV carboxylic carbon; O 1s 532.0 eV  $\pi$ -bonded oxygen, 533.6 eV  $\pi$ -bonded oxygen), (b) after a 20-min exposure to far-UV in air, and (c) after ablative photodecomposition with laser. The broken lines are mixed Gaussian-Lorentzian peaks whose sum (solid lines) gives a least-squares fit to the data points (circles).

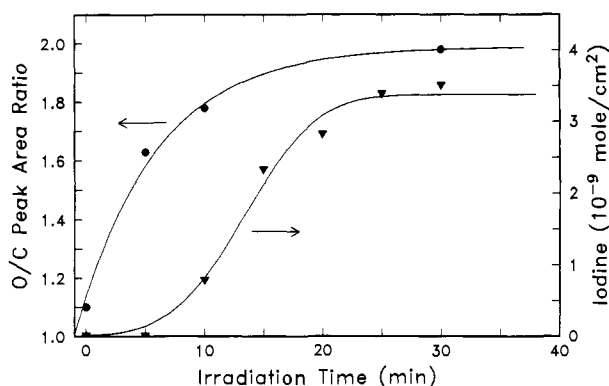


**Figure 2.** The effect of exposure of poly(ethylene terephthalate) at 185 nm in air. (●) XPS O/C area ratio as a function of irradiation time. (▼) Amount of iodine produced per  $\text{cm}^2$  of irradiated surface as a function of irradiation time.

The results of XPS studies<sup>10</sup> on a sample of poly(ethylene terephthalate) film which had been exposed to CW 185-nm radiation<sup>11</sup> are shown in Figure 1. The spectra of the C 1s and O 1s levels were resolved into individual peaks. After 10 min of irradiation the film showed substantial superficial oxidation: the O/C ratio increased by a factor of 2.0 and the C 1s peaks corresponding to single and double bonding to oxygen<sup>6</sup> are seen to increase relative to the unoxidized carbon peak at 285 eV (Figure 1). When  $\sim 140 \text{ cm}^2$  of the irradiated surface was allowed to react with 10% KI solution, free iodine was liberated, revealing the oxidizing character of the new surface. Figure 2 shows plots of the O/C peak area ratios and the oxidizing power of the surface as a function of the irradiation time. While both curves reach limiting values in a short time, they do so with different speed. The depths of the layers sampled by XPS and iodimetry are probably different, which may account for the differences in shapes of these curves.

(10) The XPS measurements were obtained with a Vacuum Generators CLAM hemispherical analyzer using  $\text{Mg K}\alpha$  (1253.6 eV) radiation at a 10-eV pass energy. The detector was  $15^\circ$  from the sample normal.

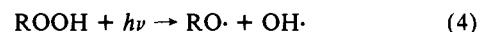
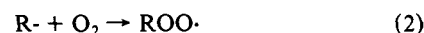
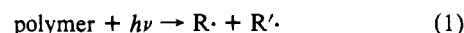
(11) CW irradiations (185 nm) were done with a BHK mercury vapor grid lamp.

**Table I.** Ratio of the Oxygen to Carbon XPS 1s Peak Areas for Poly(ethylene terephthalate) (PET), Polyimide (PI), and Poly(methyl methacrylate) (PMMA) for Various Treatments<sup>f</sup>

	<i>a</i>	<i>b</i>	<i>c</i>	<i>d</i>	<i>e</i>	
PET	1	(1.08)	2.00	1.10	1.10	0.70
PI	1	(0.70)	2.10	1.00	1.00	0.57
PMMA	1	(1.10)	1.35	1.12	1.12	1.05

<sup>a</sup> Sample as received. <sup>b</sup> Exposed 10 min to CW 185-nm irradiation in the presence of air. <sup>c</sup> Same sample as *b* subsequently soaked for 1 h in water. <sup>d</sup> Same sample as *b* subsequently reduced in a 10% KI solution. <sup>e</sup> Irradiated with three 28-ns pulses from an ArF excimer laser (193 nm) with an intensity in the range of  $150 \text{ mJ}/\text{cm}^2$ . <sup>f</sup> All are normalized to 1 for the untreated surface; <sup>g</sup> the numbers in parentheses are the measured ratios.

The mechanism proposed by Wiles and his co-workers<sup>7</sup> for the photooxidation of poly(ethylene terephthalate) in the near- and mid-UV region involves the following steps:



These reactions can also explain the surface oxidation in the far-ultraviolet if the hydroperoxide group, from which the 286.7 eV C 1s peak originates,<sup>6</sup> is identified as the source of the oxidizing power of the film. Further elementary steps are necessary to explain the etching of the film as a result of extensive photooxidation,<sup>9,12</sup> a process that proceeds at a rate of  $50 \text{ \AA}/\text{min}$ , as well as the formation of carboxylic groups seen in the XPS spectrum at 289 eV.<sup>6</sup>

In order to determine if the new surface phase is strongly bonded to the bulk, a photooxidized poly(ethylene terephthalate) film was dipped into water for 1 h prior to analysis. XPS showed a decrease (Table I) in the O/C ratio and the iodine test indicated that most, if not all, of the oxidizing power is transferred to the liquid phase. Probably a highly oxidized, nonvolatile layer is removed by wetting.<sup>13</sup> It should be emphasized that after reduction in aqueous KI (Table I, column *d*) the photooxidized surface of poly(ethylene terephthalate) still showed an oxygen content increased by  $\sim 10\%$ , indicating that new functionalities were introduced by far-UV irradiation. The chemical reaction of the modified surface will be described in a further publication.

After laser photoablation (fluence  $\sim 150 \text{ mJ}/\text{cm}^2$ ) the XPS analysis of the poly(ethylene terephthalate) sample showed a net decrease in the O/C ratio (Table I, column *e*). Thus, a carbon-rich surface is produced by treatment with the laser pulse. In addition, according to iodometry, the surface does not appear to be oxidizing. This strongly contrasts with the results of lamp irradiation at a similar wavelength and indicates that during the ablative photodecomposition oxides of carbon are expelled, while the carbon radicals remaining attached to the surface decay predominantly by C-C recombination. The stream of ablated material, which has been shown to be expelled at supersonic velocities,<sup>14</sup> probably prevents ambient oxygen from reaching the activated surface. Therefore, the carbon radicals are not trapped by oxygen.

The behavior of polyimide (condensate of pyromellitic dianhydride and *p,p'*-diaminodiphenyl oxide) and poly(methyl methacrylate) under far-UV radiation has also been examined. The O/C ratios as measured by XPS for various treatments of these polymers are compared to those obtained for poly(ethylene terephthalate) in Table I. Laser ablation of polyimide causes a greater decrease in the O/C ratio than for poly(ethylene terephthalate), whereas CW irradiation results in a comparable increase in O/C. The oxidized layer also appears to be essentially removed when rinsed. On the other hand, irradiation of poly-

(12) Srinivasan, R. *Polymer* **1982**, *23*, 1863.

(13) Wetting effect after polymer surface treatment has been reported; see ref 6b and 3a.

(14) Srinivasan, R.; Liu, S.-H. unpublished results.

(methyl methacrylate) with either UV source has little net effect on the composition of the surface. The polymer decomposes primarily into small molecules (exclusively monomer with laser ablation<sup>15</sup>) and the increase in the O/C ratio is small or zero. Even though these three polymers show somewhat different degrees of surface reaction with oxygen, they all show a high degree of specificity after far-UV oxidation, e.g., in the attachment of silver atoms to the surface.<sup>16</sup>

In summary, far-UV CW irradiation of poly(ethylene terephthalate) and polyimide in air leads to a rapid oxidation of the surface region, whereas laser ablation leads to a surface that is depleted in oxygen. Poly(methyl methacrylate) appears to be less reactive in terms of surface modification than either of these polymers.

**Registry No.** Poly(ethylene terephthalate) (SRU), 25038-59-9; poly(methyl methacrylate) (homopolymer), 9011-14-7; (*p,p'*-diaminodiphenyl oxido)-(pyromellitic dianhydride) (copolymer), 25038-81-7; poly(pyromellitic dianhydride)-(*p,p'*-diaminodiphenyl oxide) (SRU), 25036-53-7.

(15) Seeger, D.; Srinivasan, R., unpublished results.

(16) Srinivasan, R.; Jipson, V.; Poirier, M. J. *Surf. Sci. Lett.* **1983**, *130*, 344.

## Synthesis and Structure Determination of Isoaplysin-20

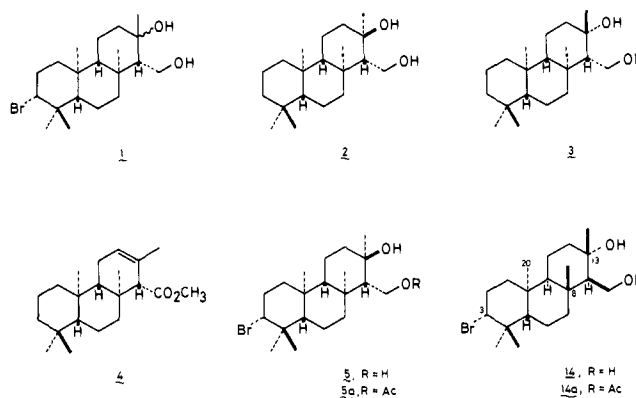
Mugio Nishizawa,\* Hideyuki Takenaka, Ken Hirotsu, Taiichi Higuchi, and Yuji Hayashi

Department of Chemistry, Faculty of Science  
Osaka City University  
Sumiyoshiku, Osaka 558, Japan  
Received March 26, 1984

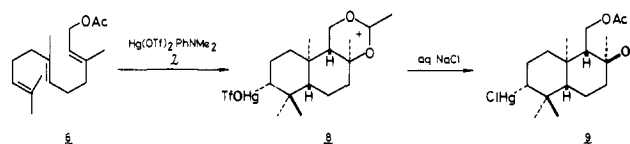
In 1977, Yamamura and Terada reported the isolation of a small amount of bromine-containing tricyclic diterpenoid, named isoplysin-20, from a sea hare, *Aplysia kurodai*.<sup>1</sup> They proposed the structure **1** to this new class of diterpenoid based on the spectral analysis, in which the stereochemistry at C-13 remained unclear. Imamura and Rūveda followed the structural study and prepared two kinds of debromo compounds (**2** and **3**) from methyl isocopalate (**4**). By comparison of the <sup>1</sup>H NMR spectra with those of the natural product, they concluded that the structure of isoplysin-20 must be represented by the formula **5**<sup>2</sup> (Chart I).

We have synthesized polycyclic terpenoids with some ambiguity in their proposed structures by means of mercury(II) trifluoromethanesulfonate/amine complex induced olefin cyclization.<sup>3</sup> As mentioned in our earlier communication,<sup>4</sup> (*E,E*)-farnesyl acetate (**6**) cyclizes by this method to a C-8 hydroxylated product, **9**, as the major product in a stereospecific manner. This is recognized as a result of intramolecular participation of the neighboring acetoxy group as represented in Scheme I. Therefore, we expected that (*E,E,E*)-geranylgeranyl acetate (**10**) would lead to the corresponding C-13 hydroxylated tricyclic product analogously. This was the case, indeed, and we prepared bromine-containing tricyclic compounds. However, the major carbinol product **5a** showed different spectral properties from those of the acetate of natural isoplysin-20. The cyclization of **10** was not completely stereospecific, and small amounts of minor products were also obtained. One of the minor products showed an entirely superimposable <sup>1</sup>H NMR spectrum with that of the natural product derivative. Single-crystal X-ray diffraction experiment gave the

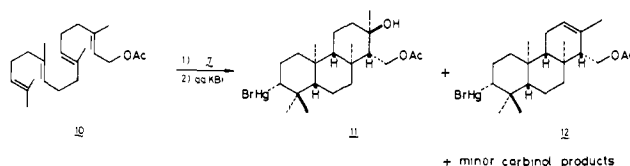
## Chart I



## Scheme I



## Scheme II



precise structure of this synthetic material (**14a**); therefore the correct structure of isoplysin-20 is shown in formula **14** with a chair/boat/chair perhydrophenanthrene skeleton.

Treatment of (*E,E,E*)-geranylgeranyl acetate (**10**)<sup>5</sup> with mercury(II) trifluoromethanesulfonate/*N,N*-dimethylaniline complex (**7**) (1.2 equiv) in nitromethane at  $-20^{\circ}\text{C}$  for 2 h,<sup>4</sup> and subsequent exposure to an aqueous solution of KBr (excess) at room temperature for 12 h afforded a *tert*-alcohol product, **11** (mp 222–223  $^{\circ}\text{C}$ , 16% yield), together with an olefinic compound, **12** (mp 188.5–190  $^{\circ}\text{C}$ , 17% yield)<sup>6</sup> (Scheme II). The stereochemistry of **11** was rigidly established by the conversion to the demercuration product **2** ( $\text{NaBH}_4/\text{aqueous NaOH}/\text{C}_2\text{H}_5\text{OH}$ ),<sup>7</sup> which was identified with the compound reported by Rūveda.<sup>2</sup> The organomercury compound **11** was then subjected to the bromination according to the procedure reported by Hoye ( $\text{Br}_2/\text{LiBr}/\text{O}_2/\text{pyridine}$ )<sup>8</sup> to give **5a** in 65% yield (mp 166.5–167  $^{\circ}\text{C}$ ). The orientation of C-3 bromine was clearly shown to be  $\alpha$ -equatorial based on its <sup>1</sup>H NMR spectrum (H-3:  $\delta$  3.94, dd,  $J = 12$  and 4 Hz). However, this spectrum showed a different pattern in the methyl region ( $\delta$  0.86 (6 H), 0.94 (3 H), 1.05 (3 H), and 1.16 (3 H)) from that of natural isoplysin-20 acetate ( $\delta$  0.92 (3 H), 0.97 (3 H), 1.03 (6 H), and 1.20 (3 H)). Thus, the structure of isoplysin-20 is not **5**, which was proposed by Rūveda.<sup>2</sup>

Now we turned our attention to the minor products of the above hydroxylative cyclization. After separation of the major carbinol product **11**, the presence of some minor stereoisomeric constituents were detected in the crystallization mother liquor. This mixture was subjected to bromination as mentioned before and exhaustive purification by using HPLC.<sup>9</sup> Two kinds of tricyclic compounds, **13** (mp 147  $^{\circ}\text{C}$ , 1.6% yield from **10**)<sup>10</sup> and **14a** (mp 178  $^{\circ}\text{C}$ , 1.8%

(1) Yamamura, S.; Terada, Y. *Tetrahedron Lett.* **1977**, 2171.

(2) Imamura, P. M.; Rūveda, E. A. *J. Org. Chem.* **1980**, *45*, 510.

(3) Nishizawa, M.; Takenaka, H.; Hayashi, Y. *Tetrahedron Lett.* **1984**, *25*, 437.

(4) Nishizawa, M.; Takenaka, H.; Nishide, H.; Hayashi, Y. *Tetrahedron Lett.* **1983**, *24*, 2581.

(5) Stereochemical purity of starting (*E,E,E*)-geranylgeraniol is assayed to be >99% pure according to GLC and HPLC analysis.

(6) Nishizawa, M.; Takenaka, H.; Hayashi, Y. *Chem. Lett.* **1983**, 1459.

(7) Hoye, T. R.; Caruso, A. J.; Kurth, M. J. *J. Org. Chem.* **1981**, *46*, 3550.

(8) Hoye, T. R.; Kurth, M. J. *J. Org. Chem.* **1979**, *44*, 3461.

(9) Acetonitrile/water (7:3) on a Develosil ODS-5 column and then hexane/ethyl acetate (3:1) on a Develosil Silica 30-3 column using an Altex RI detector.